

# Enhanced Microlensing by Stars Around the Black Hole in the Galactic Center

Tal Alexander

Institute for Advanced Study, Olden Lane, Princeton, NJ08540<sup>1</sup>

and

Abraham Loeb

Harvard-Smithsonian Center for Astrophysics, 60 Garden Street, Cambridge, MA 02138

The effect of stars on the lensing properties of the supermassive black hole in the Galactic Center is similar to the effect of planets on microlensing by a star. We show that the dense stellar cluster around SgrA\* enhances by up to an order of magnitude the probability of high-magnification lensing events of a distant background source by the black hole. Conversely, the gravitational shear of the black hole changes and enhances the microlensing properties of the individual stars. The effect is largest when the source image lies near the Einstein radius of the black hole ( $1.75'' \pm 0.20''$  for a source at infinity). We estimate that the probability of observing at least one distant background star which is magnified by a factor  $> 5$  in any infrared snapshot of the inner  $\sim 3''$  of the Galactic Center is  $\sim 20\%$  with present-day photometric sensitivity. Deeper future photometry will significantly increase the number of detected images. The largest source of uncertainty in this estimate is the luminosity function of the background stars. The gravitational shear of the black hole lengthens the duration of high-magnification events near the Einstein radius up to a few months, and introduces a large variety of lightcurve shapes that are different from those of isolated microlenses. Identification of such events by image subtraction can be used to probe the mass function, density and velocity distributions of faint stars near the black hole, which are not detectable otherwise.

*Subject headings:* Galaxy: center — gravitational lensing — infrared: stars — Galaxy: stellar content

## 1. Introduction

Deep infrared observations of the innermost region around the massive black hole (BH) in the Galactic Center (GC) reveal numerous point sources (Genzel et al. 1997; Ghez et al. 1998). Most of these are probably stars orbiting deep in the potential of the BH. However, the BH will also gravitationally lens and magnify any background star that happens to lie behind it, and so a small fraction of these point sources could be lensed images of distant background stars. The possible existence of such images in the innermost GC, beyond being a probe of the BH potential, may also affect the apparent star counts, radial stellar density distribution and infrared luminosity

---

<sup>1</sup>Present address: Space Telescope Science Institute, 3700 San Martin Drive, Baltimore, MD 21218

function. Previous investigations of gravitational lensing by the BH (Wardle & Yusef-Zadeh 1992; Alexander & Sternberg 1999) suggested that lensing effects do not play a major role in present-day observations of the GC. However, the BH is surrounded by a very dense stellar cluster (e.g. Genzel et al. 1997), whose contribution to the lensing by the BH has so far been neglected. Because the stellar mass is not smoothly distributed around the BH but is composed of discrete point masses, its effect on the lensing properties of the BH is much larger than one may naively estimate by adding the stellar mass to that of the BH.

The effect of a star on lensing by the BH is analogous to the effect of a planet on microlensing by its star. The latter problem has been studied in great detail in the context of microlensing searches for planets (Mao & Paczynski 1991; Gould & Loeb 1992; Bolatto & Falco 1994; Gaudi & Gould 1997; Wambsganss 1997; Peale 1997; Griest & Safizadeh 1998; Gaudi, Naber, & Sackett 1998; Gaudi & Sackett 1997). In particular, Gould & Loeb (1992) first showed that the cross-section for magnification by the planet can be increased by up to an order of magnitude due to the gravitational shear of the star; the effect being most pronounced when the planet lies near the Einstein radius of the star. Aside from the change in scales, the same result should apply to SgrA\*. In the GC, the primary massive lens is the BH and the secondary low-mass lenses are the stars around it. If a star happens to pass near the image of a source that is being lensed by the BH, then the magnification of the image could be enhanced significantly. The BH shear increases the probability for high magnification events by individual stars. In this paper we calculate the probability of high-magnification events in the stars-BH system and compare it to the naked BH case.

The statistics of microlensing by stars in the GC region is very different from that in the Galactic disk or halo. In the latter case, the optical depth for microlensing is very small,  $\tau \sim 10^{-7}$ – $10^{-5}$ , but there are many background sources (see, e.g. review by Paczynski 1996). In contrast, the optical depth for microlensing by stars within the inner arcsecond of the GC is as high as  $\sim 0.1$  due to the high stellar density there (see §4), but it is not clear whether there is a sufficient number of bright background sources. In fact, due to their large distances and high extinction by dust, most sources behind the GC will only be observable while being magnified during a lensing event. The microlensing events are transient; any distant source behind the GC will be microlensed for a fraction of the time due to foreground stars which are passing in front of its images.

This paper is organized as follows. The method of our calculation is described in §2; the models of the stellar lenses and background stellar sources are described in §3; and the numerical results are presented in §4. We discuss the main implications of our results in §5.

## 2. Method

We adopt the semi-analytic method of Gould & Loeb (1992; see also the original discussion by Chang & Refsdal 1979, 1984) to describe the effect of a low-mass secondary lens (a star) on the image produced by a high-mass primary lens (the BH). We consider rare, high-magnification events for which the possibility that more than one star affects the microlensing event at any given time can be neglected. The original, unperturbed image position at  $\mathbf{x}_{i\bullet}$  is displaced by  $\boldsymbol{\xi}_i = (\xi_i, \eta_i)$  due to the perturbing star at a position  $\boldsymbol{\xi}_p = (\xi_p, \eta_p)$  relative to the unperturbed image. We express the source position  $\mathbf{x}_s$  and the unperturbed image position  $\mathbf{x}_{i\bullet}$  in terms of the Einstein angular radius of the isolated BH,

$$\theta_E \equiv \left[ \frac{4GM_\bullet (D_s - R_0)}{c^2 D_s R_0} \right]^{1/2} = (1.75'' \pm 0.20'') \times \left( 1 - \frac{R_0}{D_s} \right)^{1/2}, \quad (1)$$

where  $M_\bullet = (3.0 \pm 0.5) \times 10^6 M_\odot$  (Genzel et al. 2000) is the BH mass,  $R_0 = 8.0 \pm 0.5$  kpc (Reid 1993) is the distance to the GC, and  $D_s$  is the distance to the source ( $1'' \simeq 0.04$  pc at the GC). We express the displacement vectors  $\boldsymbol{\xi}_i$  and  $\boldsymbol{\xi}_p$  in terms of the Einstein radius of the star,  $\sqrt{\epsilon}\theta_E$ , where  $\epsilon = m_\star/M_\bullet$  is the mass ratio between the star and the BH. This quantity provides a good measure for the scale of the stellar lensing zone. Correspondingly, we express areas in the lens plane,  $\sigma_\star$ , in units of  $\epsilon\pi\theta_E^2$ , the Einstein ring area of an isolated star; and normalize surface number densities of lensing stars in the lens plane,  $\Sigma_\star$ , by  $(\epsilon\pi\theta_E^2)^{-1}$ . Areas in the source plane,  $\sigma_s$ , are expressed in terms of  $\pi\theta_E^2$ , and surface number density of sources in the source plane,  $\Sigma_s$ , are correspondingly expressed in terms of  $(\pi\theta_E^2)^{-1}$ .

In the limit  $\epsilon \ll 1$ ,  $\xi_i$  is given by the two or four solutions to the equations (Gould & Loeb 1992)

$$\begin{aligned} \xi_i^4 + \frac{(1-2\gamma)\xi_p}{\gamma}\xi_i^3 + \left[ \frac{(1-\gamma)^2(\xi_p^2 + \eta_p^2)}{4\gamma^2} - \frac{(1-\gamma)\xi_p^2}{\gamma} - \frac{1}{1+\gamma} \right] \xi_i^2 - \\ \left[ \frac{(1-\gamma)^2(\xi_p^2 + \eta_p^2)\xi_p}{4\gamma^2} + \frac{(1-\gamma)\xi_p}{\gamma(1+\gamma)} \right] \xi_i - \frac{(1-\gamma)^2\xi_p^2}{4\gamma^2(1+\gamma)} = 0, \end{aligned} \quad (2)$$

where  $\gamma \equiv x_{i\bullet}^{-2}$ , and

$$\eta_i = \frac{(1+\gamma)\eta_p\xi_i}{2\gamma\xi_i + (1-\gamma)\xi_p}. \quad (3)$$

The magnification of each of the images is

$$A = \left| 1 - \left[ \gamma + (1+\gamma)^2\xi_i^2 - (1-\gamma)^2\eta_i^2 \right]^2 - 4(1-\gamma)^2\xi_i^2\eta_i^2 \right|^{-1}. \quad (4)$$

For the GC, we consider solar mass lenses and adopt, for simplicity, a single value of  $\epsilon = 3 \times 10^{-7}$ .

The angular area in the source plane where a background source would be magnified above a given threshold  $A$  by the star-BH system,  $\sigma_s(>A)$ , is obtained by identifying the corresponding

angular area in the lens plane around the unperturbed image and transforming it back to the source plane<sup>2</sup>. The lensing stars are distributed randomly around the BH and they scan the lens plane as they move. Averaging over time and assuming an isotropic projected stellar distribution around the BH,

$$\sigma_s(> A) = \frac{1}{\pi} \int P(> A, \mathbf{x}_{i\bullet}) \left| \frac{d\mathbf{x}_s}{d\mathbf{x}_{i\bullet}} \right| d\mathbf{x}_{i\bullet} = 2 \int P(> A, \mathbf{x}_{i\bullet}) A_\bullet^{-1}(\mathbf{x}_{i\bullet}) x_{i\bullet} d\mathbf{x}_{i\bullet}, \quad (5)$$

where  $P(> A, \mathbf{x}_{i\bullet})$  is the probability for magnification above  $A$ , that is, the fraction of  $d\mathbf{x}_{i\bullet}$  where the image is magnified above  $A$ . Equivalently,  $P(> A, \mathbf{x}_{i\bullet})$  is the fraction of time a stationary source is magnified above  $A$  by a closely-passing star. The magnification  $A_\bullet$  is that due to the BH alone,

$$A_\bullet = \left| \frac{d\mathbf{x}_{i\bullet}}{d\mathbf{x}_s} \right| = \left| 1 - x_{i\bullet}^{-4} \right|^{-1}, \quad (6)$$

where the positions of these images are related to the source position,

$$x_{i\bullet, \pm} = \frac{1}{2} \left( x_s \pm \sqrt{x_s^2 + 4} \right). \quad (7)$$

De-magnification, i.e.  $A < A_\bullet$ , is also possible. The probability  $P$  is expressed in terms of the optical depth

$$\tau_\star(> A, x_{i\bullet}) \equiv \Sigma_\star(x_{i\bullet}) \sigma_\star(> A, x_{i\bullet}), \quad (8)$$

where  $\sigma_\star(> A, x_{i\bullet})$  is the area in the lens plane where the presence of a star will lead to magnification above  $A$ , and  $\Sigma_\star(x_{i\bullet})$  is the stellar lens surface density. In the small optical depth limit

$$P(> A, \mathbf{x}_{i\bullet}) \simeq \tau_\star(> A, x_{i\bullet}) + \Theta(A_\bullet - A), \quad (9)$$

where  $\Theta$  is the Heaviside step function. In practice, the lens plane area  $\sigma_\star(> A, x_{i\bullet})$  is calculated by solving Eqs (2)–(4) numerically as functions of  $\xi_p$  in a small test area  $\sigma_0(x_{i\bullet})$  around  $\mathbf{x}_{i\bullet}$  where the effect of the stellar lens magnification is appreciable. The effect of the star outside of  $\sigma_0$  is neglected. With this assumption, the probability for not being affected by any star is  $\exp(-\tau_0)$ , where  $\tau_0 \equiv \Sigma_\star \sigma_0$ . The magnification probability is then given by the sum of the probabilities of magnification by a star or by the BH alone,  $P(> A) = [1 - \exp(-\tau_\star)] + \exp(-\tau_0) \Theta(A_\bullet - A)$ , which in the limit  $\tau_\star \ll 1$  reduces to Eq. (9), independently of the exact choice of  $\sigma_0$ .

For an isolated BH ( $\Sigma_\star = 0$ ), the corresponding angular area in the high magnification limit,  $A \gg 1$ , is  $\sigma_s(> A) \approx 1/2A^2$ .

Equations (2)–(4) are valid as long as  $\tau_\star(> A, x_{i\bullet}) \ll 1$ , i.e. when  $A$  is large enough so that there is no overlap between the regions of influence (lensing zones) of different stars,  $\sigma_\star(> A, x_{i\bullet}) \ll \Sigma_\star^{-1}(x_{i\bullet})$ . In addition, these equations ignore the cumulative effect of all the stars on the central caustic around the BH (Griest & Safizadeh 1998). For  $\epsilon = 3 \times 10^{-7}$ , the central

---

<sup>2</sup> Source areas that contribute two images which are above the magnification threshold, are counted twice.

caustic has a negligible contribution to the integrand of Eq. (5) as long as  $x_{i\bullet}$  is not very close to unity (i.e. for sources which are not located almost behind the BH). The inclusion of the central caustic can only increase our estimated lensing probabilities.

### 3. Model

In §4 below we demonstrate the effect of enhanced microlensing by stars near a massive BH by calculating the mean number of lensed images with magnification above a threshold  $A$ ,  $\langle N_i(>A) \rangle = \sigma_s(>A)\Sigma_s$ , of distant background sources behind SgrA\*. To do this, we need to specify the projected density of the stellar lenses  $\Sigma_*$ , which determines the optical depth for microlensing and hence the cross-section in the source plane  $\sigma_s(>A)$ , and we also need to specify the projected source density  $\Sigma_s$ .

#### 3.1. Stellar Lenses Around SgrA\*

The stellar mass density distribution near the BH is modeled as a power-law,

$$\rho = (3 - \alpha)\rho_b \left(\frac{r}{r_b}\right)^{-\alpha}, \quad (10)$$

with  $\rho_b = 10^6 M_\odot \text{pc}^{-3}$ ,  $r_b = 0.4 \text{pc}$  and an index  $\alpha$  in the range of  $3/2$ – $7/4$ . This distribution is indicated by an analysis of the star counts in the inner GC (Alexander 1999) and agrees with the theoretical prediction for a relaxed stellar system around a black hole (Bahcall & Wolf 1977), as is thought to be the case in the GC. For simplicity, we assume that the stellar lenses all have the same mass  $m_* = 1 M_\odot$  ( $\epsilon \approx 3 \times 10^{-7}$ ). For these low mass stars, we adopt the theoretical prediction of  $\alpha \sim 3/2$ . The corresponding surface mass density (in units of  $M_\bullet / \pi\theta_E^2$ ) and surface number density (in units of  $1/\epsilon\pi\theta_E^2$ ) at an angular separation  $x = \theta/\theta_E$  from the GC are both given by  $\Sigma_* = \hat{\Sigma}_* x^{1-\alpha}$ , with  $\hat{\Sigma}_* \simeq 0.035$ . The normalization  $\hat{\Sigma}_*$  is almost independent of  $\alpha$  in the above range and scales with  $\theta_E$  and  $M_\bullet$  as  $\theta_E^{3-\alpha} / M_\bullet$ . The ratio of stellar mass enclosed within the Einstein radius and the mass of the BH is  $2\hat{\Sigma}_*/(3-\alpha)$ . Note that  $\Sigma_*$  is also the optical depth for lensing by the stars alone, neglecting the effect of the BH. As we show below, the actual optical depth increases substantially when the shear of the BH is included, an effect analogous to the cross-section enhancement for planetary systems (Gould & Loeb 1992).

#### 3.2. Distant Background Stars

A rough estimate of the projected density of distant stars, which is based on a model of the  $K$ -band luminosity distribution in the Galaxy (Kent 1992) and the assumption that the mean mass-to-light ratio is solar, suggests that there are of order  $\sim 100$  distant background stars within

$\sim 2''$  of the BH. We define “distant background stars” as those stars with  $\theta_E \gtrsim 1''$ , i.e. farther than  $\sim 4$  kpc behind the BH. The surface density of nearby background stars in the inner bulge and in the high density central cluster may be as high as  $\sim 10^3$  arcsec $^{-2}$  (Alexander & Sternberg 1999). However, the Einstein angular radius for stars so close behind the BH is less than  $0.1''$  and there are not enough lensing stars near the BH on that scale for microlensing to become important. Here, we study the role of these close stars as microlenses rather than as sources.

Another way of estimating  $\Sigma_s$  is to extrapolate to low luminosity the observed stellar  $K$  luminosity function (KLF) in the  $b = 0^\circ$ ,  $l = 30^\circ$  direction (i.e. impact parameter of 4 kpc relative to the GC) and correct it for projection, foreground stars and the higher extinction at  $l = 0^\circ$ . The infrared Galactic model of Ortiz & Lépine (1993), which reproduces such observations, predicts  $\Sigma_s(< 13^m) \sim 0.1$  (see their Fig. 17b) with a steep slope of  $b \equiv d \log \Sigma_s / dK \sim 0.4$  to 0.5. The projected stellar population is integrated over most of the Galactic disk and is composed of stars of different ages, and so it is reasonable to approximate it as an old, continuously star forming population. Observations of such populations in the Galactic Bulge (Tiede et al. 1995; Holtzman et al. 1998) and the central cluster in the GC (Blum, Sellgren & DePoy 1996; Davidge et al. 1997), as well as stellar population synthesis of the GC (Alexander & Sternberg 1999), indicate that the post-main-sequence KLF, where the  $K$ -luminous sources lie, typically takes the form of a single power-law with  $b \sim 0.3$ – $0.4$  down to the main sequence turn-off point at  $M_{K_{ms}} \gtrsim 3.5^m$ , where the power-law flattens and then turns over. The Galactic extinction model of Wainscoat et al. (1992) predicts that the integrated  $K$ -band extinction in the direction of the GC is  $\sim 2^m$  larger than that at  $l = 30^\circ$ . The correction for foreground stars and for the projection from  $l = 30^\circ$  to  $l = 0^\circ$  (assuming an exponential Galactic disk with a length scale of 3.5 kpc, Wainscoat et al. 1992) further reduces the projected density by a factor of  $\sim 0.5$ . We include these corrections by adopting the normalization  $\Sigma_s(< 15^m) \sim 0.05$  for the distant background stars. The uncertainty in the exact shape of the luminosity function, the patchiness of the extinction in the Galactic Plane, and the distribution of star-forming regions in the spiral arms behind the GC introduce a large uncertainty to  $\Sigma_s$ . Putting these uncertainties aside, we adopt a working model for the KLF of the distant background stars,

$$\Sigma_s(< K) = \hat{\Sigma}_s 10^{bK}, \quad (11)$$

with  $\hat{\Sigma}_s = 5 \times 10^{-8}$  and  $b = 0.4$ . Assuming a typical distance of  $2R_0$  to the distant background sources and  $A_K \sim 3.5^m$  to the GC (Blum et al. 1996), the power-law KLF extends down to the main-sequence turn-off at  $K_{ms} \sim 25^m$ . This KLF corresponds to a  $\Sigma_s(< K_{ms})$  value of order a few hundred, in rough agreement with the value derived from the Galactic  $K$ -luminosity density model.

The differential surface density of lensed stars,  $d\tilde{\Sigma}_s/d\tilde{F}|_{\tilde{F}}$ , is related to their unlensed luminosity function by  $d\tilde{\Sigma}_s/d\tilde{F}|_{\tilde{F}} = A^{-2} d\Sigma_s/dF|_{F/A}$ , where the tilde denotes lensed quantities and where  $d\Sigma_s/dF|_F \propto F^{-2.5b-1} \propto F^{-2}$  for the KLF of Eq. (11). Hence, the adopted surface density has the critical power-law slope for which the differential flux distribution remains unchanged.

## 4. Results

Figure 1a shows the integrated source plane area  $\sigma_s(> A)$  for producing a lensed image magnified by more than  $A$  anywhere in the inner  $2\theta_E$ . The highest magnifications are due to stellar lenses close to  $\theta_E$ . The results are presented only up to  $A = 100$  and the integration range in Eq. (5) does not include the annulus  $|1 - x_{i\bullet}| < \delta x = 0.005$ , because at that point the change in  $A_\bullet$  over the angular scale defined by  $\sigma_\star(> A, x_{i\bullet})$  is no longer small,  $\sqrt{\sigma_\star(> 100, x_{i\bullet})} \gtrsim \delta x$ , and the semi-analytic approximation (Eq. 4) no longer applies. We verified the validity of our semi-analytic calculations for the case of a BH and a single star in the range  $\delta x > 0.001$  by comparing  $\sigma_\star(> A, x_{i\bullet})$  as function of  $A$  and  $x_{i\bullet}$ , with results from the direct ray shooting method (Wambsganss & Kubas 2000). The two methods give identical results to within  $\sim 5\%$  down to  $\delta x = 0.1$  for both the normalization and slope and remain in good qualitative agreement even down to  $\delta x = 0.001$  throughout the range where the ray-shooting method has sufficiently high resolution. Although  $\tau_\star(> A, x_{i\bullet}) \ll 1$  no longer holds for  $A < 100$  as  $\sigma_\star(> A, x_{i\bullet})$  increases near  $x_{i\bullet} \pm \delta x$ , this should not introduce a large error in  $\sigma_s(> A)$  since the relative contribution from these regions to all but the highest magnification falls off rapidly as  $A_\bullet^{-1}$  (Eq. 5 and Fig. 1b).

Figure 1b shows the differential area  $d\sigma_s(> A)/dx_{i\bullet}$ , for the BH with and without the stars. Both  $\sigma_s(> A)$  for the BH alone and  $d\sigma_s(> A)/dx_{i\bullet}$  for the BH and stars (not plotted here) fall off as  $A^{-2}$  for  $A \gg 1$  at any  $x_{i\bullet} \neq 1$ , in accordance with the theoretical asymptotic limit for a point source (Schneider, Ehlers & Falco 1992). In contrast,  $\sigma_s(> A)$  for the BH and stars falls off only as  $A^{-3/2}$  up to  $A \sim 100$ , and only then does it start converging to the asymptotic  $A^{-2}$  scaling. While the truncation at  $x_{i\bullet} = 1 \pm \delta x$  introduces a maximum magnification factor for the naked BH case,  $A_{\max} \sim 50$ , the tail of high magnifications is not bounded for the BH+stars system. Even for magnifications  $A \ll A_{\max}$ , the cross-section of the BH+stars system is larger by factors of  $\sim 3$ , depending on the normalization of the surface density model for the lensing stars. The profile of  $d\sigma_s(> A)/dx_{i\bullet}$  versus  $x_{i\bullet}$  (Fig. 1b) shows that the contribution of stars to the high magnification events extends well beyond the narrow region around the Einstein radius that is expected for an isolated BH.

Figure 2a shows the number of lensed images that will be observed, on average, in the inner  $2\theta_E$  for different limiting  $K$ -magnitudes, assuming the KLF of Eq. (11),

$$\begin{aligned} \langle N_i(> A; K_0) \rangle &= \int_A^\infty dA' \int_{-\infty}^{K_0} dK \left. \frac{d\sigma_s}{dA} \right|_{A'} \left. \frac{d\Sigma_s}{dK} \right|_{K+K_{A'}} \\ &= \hat{\Sigma}_s \hat{\sigma}_s \begin{cases} 10^{bK_{\text{ms}}} A_{\text{ms}}^{-1.5} + \frac{3}{5b-3} 10^{bK_0} \left( A_{\text{ms}}^{2.5b-1.5} - A^{2.5b-1.5} \right) & \text{if } A \leq A_{\text{ms}} \\ 10^{bK_{\text{ms}}} A^{-1.5} & \text{else} \end{cases}, \end{aligned} \quad (12)$$

where we assume that the KLF has a sharp cutoff beyond  $K_{\text{ms}}$ , and where  $K_A \equiv 2.5 \log A$ ,  $A_{\text{ms}} \equiv 10^{0.4(K_{\text{ms}} - K_0)}$ , and  $\sigma_s$  is parameterized as  $\sigma_s(> A) = \hat{\sigma}_s A^{-1.5}$  with  $\hat{\sigma}_s \approx 0.5$  for  $\hat{\Sigma}_\star = 0.06$  (Fig. 1a). An analogous expression with  $A^{-2}$  and a lower normalization describes the magnification by the BH alone. For low values of  $A$  and  $K_0$ ,  $\langle N_i(> A; K_0) \rangle$  decreases slowly like  $\propto A^{2.5b-1.5}$  because the decrease of  $\sigma_s(> A)$  is partially offset by the ever larger number of faint stars in the

population that become accessible. However, once  $K_0 + K_A > K_{\text{ms}}$ , all the background stellar population can be observed when magnified by  $A$ , and  $\langle N_i(> A; K_0) \rangle$  falls off more rapidly, like  $\sigma_s(> A) \propto A^{-1.5}$ .

The motions of the stellar lenses and the sources introduce time-dependent Poissonian fluctuations in  $N_i(> A; K_0)$ . The fraction of time that at least one lensed image will be observed, which is shown in Fig. 2b, is  $P[N_i(> A; K_0) \geq 1] = 1 - \exp[-\langle N_i(> A; K_0) \rangle]$ . Present-day observations reach a depth of  $K_0 \sim 17^{\text{m}}$  (Ghez et al. 1998). For this threshold, at least one distant background star with  $A > 5$  is observable for  $\sim 20\%$  of the time in the inner  $2\theta_E \sim 3.5''$ , and at least one star with  $A > 100$  is observable for  $\sim 5\%$  of the time. The lensing statistics will improve significantly with deeper observations. We predict that in any snapshot of the central  $3''$  region around the GC to a  $K$ -magnitude limit of  $21^{\text{m}}$ , about one distant background star will be magnified by a factor  $> 50$ , and  $\sim 10$  will be magnified by a factor of  $> 5$ .

Variability offers a direct way of identifying the lensed images among the many foreground stars. Any source detected with a magnitude  $K_0$  at a *given* position  $x_{i\bullet}$  will be magnified by an additional factor of  $\geq A$  for a fraction  $\sim 1/A^2$  of the time (Schneider et al. 1992). Hence, continuous monitoring of detected sources would allow identification of microlensing events. Such events can be distinguished from variability of the source stars or from variable patchiness in the dust obscuration, through their achromaticity and their generic set of possible time profiles. The determination of the microlensing probability and duration distribution can be used to constrain the density and velocity distribution of low-mass stars in the GC. We demonstrate this connection qualitatively by defining a typical timescale for magnification by more than  $A$  as  $t(> A) \equiv \sqrt{\sigma_\star(> A)}/v_\perp \propto \sqrt{m_\star}/v_\perp$  (Although the actual event duration depends on the complex caustics geometry, we use this definition as a crude estimate). The projected rms transverse velocity of the low mass stellar lenses in the GC is (Alexander 1999)

$$v_\perp^2 \approx 0.37 \frac{GM_\bullet}{p}, \quad (13)$$

where  $p = \theta R_0$  is the projected distance from the BH. Figure 3 compares  $t(> A)$  of magnified images of stationary sources lensed by solar mass stars in the shear field of SgrA $^\star$  with the timescale of lensing by isolated stars (with the same velocity field). The duration of a microlensing event strongly depend on the position of the image, and is increased from several weeks to several months near  $\theta_E$ . The formal divergence of  $t(> A)$  near  $\theta_E$  is truncated in practice by the rapidly decreasing probability of having a source with an image close to  $\theta_E$  (cf Fig. 1b) and by the motion of the source, which is neglected here. Nevertheless, a sharp increase of the microlensing timescales is expected near  $\theta_E$ . In contrast with timescales of lensing by isolated stars, the timescales inside  $\theta_E$  fall rapidly to zero in the presence of the BH because the strong de-magnification by the BH (Eq. 7) has to be compensated by very high stellar lens magnification. The lensed lightcurves should show complex structures, unlike the symmetric smooth lightcurves of an isolated point mass lens. Examples of such lightcurves can be found in the literature (Mao & Paczynski 1991; Gould & Loeb 1992; Bolatto & Falco 1994, and in particular Wambsganss 1997).

## 5. Discussion and Summary

The presence of a dense stellar cluster around a super-massive BH changes considerably the lensing properties of both the stars and the BH: the magnification cross-section, the magnification probability, the variability timescale and the lightcurve structure. The modification of the microlensing properties of the stars is most pronounced near the Einstein radius of the BH. Previous work on lensing by the BH alone (Wardle & Yusef-Zadeh 1992; Alexander & Sternberg 1999) focused on stellar sources from the inner central cluster, for which  $\theta_E \sim 0.02''$ . Here we have considered lensing of distant background stars by the BH and the stars around it, for which the angular scale is  $\theta_E \sim 2''$ .

We applied our calculations to the BH and the dense central cluster in the GC, and found that the lensing probability is increased over that of an isolated BH by factors ranging from a few for low magnifications ( $\gtrsim 5$ ) up to an order of magnitude for high magnifications ( $\gtrsim 100$ ). We estimate that in any snapshot of the central  $3''$  region around the GC to a  $K$ -magnitude limit of  $21^m$ , about one distant background star will be magnified by a factor  $\gtrsim 50$ , and about ten will be magnified by a factor of  $\gtrsim 5$ . The duration of a microlensing event can be lengthened by an order of magnitude near the Einstein radius of the BH. Moreover, the gravitational shear of the BH changes considerably the shape of the microlensing lightcurves so that they are no longer symmetric and smooth as they are for isolated stars.

Variability provides the distinguishing signature of microlensed stars. Image subtraction can be used to pick out lensed images of distant background sources from the many foreground stars. The achromaticity of the lightcurves and their generic (non-periodic) temporal structures can be used to separate them from those of intrinsically variable stars. Since the variability timescale scales as  $\sqrt{m_\star}/v_\perp$ , the lightcurves contain information on the stellar mass function, the stellar density, and the stellar velocity dispersion as functions of the projected distance from the BH. In particular, the lensing timescales could probe mass segregation deep in the potential of the BH. The vast majority of the stellar lenses are low-mass faint stars that are many magnitudes dimmer than the current detection limit. Microlensing can probe the statistical properties of these yet unobserved stars.

It is important to note that our quantitative results are subject to a number of approximations and uncertainties. For the sake of simplicity, we ignored the fact that the background stars may have a broad distribution of distances and hence different values for the Einstein radius. In addition, the model for the surface density and luminosity function of the distant background stars suffers from large uncertainties given the quality of present-day data. We also ignored the contribution of blended light from the lensing star to the inferred flux from the source. However, this contribution is likely to be small for bright sources and low-mass lenses. Lastly, the semi-analytical formalism for calculating the magnification is not valid very near  $\theta_E$  and so our quantitative predictions for  $\langle N_i(> A) \rangle$  are less reliable for very high values of  $A$ . More precise calculations, for example by the ray-shooting method (Wambsganss 1997; Wambsganss & Kubas

2000) will be required to improve the accuracy of the predictions.

Finally, we emphasize that our calculations can be applied to any extragalactic supermassive black hole. For example, the core of M87 harbors a black hole mass of  $\sim 2 \times 10^9 M_\odot$ . The Einstein radius of this black hole for sources at infinity is  $\sim 2''$ , close to that of SgrA\*, and there is no sign for obscuration by dust within its boundary. However, it is more likely that the sources will be stars in M87 a few kpc behind the black hole, for which  $\theta_E \sim 0.03''$ . For the higher black hole mass in M87,  $\epsilon \sim 5 \times 10^{-10}$  and so microlensing events of stellar sources which are embedded in that galaxy will have durations comparable to those around SgrA\* since  $t \sim (\epsilon/M_\bullet)^{1/2} (D_l \theta_e)^{3/2}$ , where  $D_l$  is the distance from the observer to the BH. Since crowding and flux sensitivity severely limit the detection of individual stars at the distance of M87, one may search for microlensing of surface brightness fluctuations, the so-called pixel lensing (see, e.g. Gould 1996). The Next Generation Space Telescope (*NGST*; <http://ngst.gsfc.nasa.gov/>), with its sub-nJy sensitivity in the wavelength band of  $\sim 1\text{--}3.5\mu\text{m}$  and its  $\sim 0.06''$  resolution, is ideally suited for such a study.

We thank Joachim Wambsganss for communicating results from ray-shooting calculations prior to publication (Wambsganss & Kubas 2000). AL thanks the Institute for Advanced Study for its kind hospitality during the initiation of this paper. This work was supported in part by NASA grants NAG 5-7768, 5-7039 and NSF grants AST-0071019, AST-0071019 (for AL).

## REFERENCES

- Alexander, T., 1999, *ApJ*, 520, 137
- Alexander, T., & Sternberg, A., 1999, *ApJ*, 520, 137
- Bahcall, J. N., & Wolf, R. A., 1977, *ApJ*, 216, 883
- Blum R. D., Sellgren, K. & DePoy, D. L., 1996, *ApJ*, 470, 864
- Bolatto, A. D., & Falco, E. E., 1994, *ApJ*, 436, 112
- Chang, K. & Refsdal, S., 1979, *Nature*, 282, 561
- , 1984, *A&A*, 132, 168
- Davidge, T. J., Simons, D. A., Rigaut, F., Doyon, R., & Crampton, D., 1997, *AJ*, 114, 2586
- Gaudi, B. S., & Gould, A., 1997, *ApJ*, 486, 85
- Gaudi, B. S., Naber, R. M., & Sackett, P. D. 1998, *ApJ*, 502, L33
- Gaudi, B. S., & Sackett, P. D., 2000, *ApJ*, 528, 56
- Genzel, R., Eckart, A., Ott, T., & Eisenhauer, F., 1997, *MNRAS*, 291, 21

- Genzel, R., Pichon, C., Eckart, A., Gerhard, O. E., & Ott, T., 2000, MNRAS, 317, 418
- Ghez, A. M., Klein, B. L., Morris, M., & Becklin, E. E., 1998, ApJ, 509, 678
- Gould, A., 1996, ApJ, 470, 201
- Gould, A. & Loeb, A., 1992, ApJ, 1992, 396, 104
- Griest, K., & Safizadeh, N., 1998, ApJ, 500, 37
- Holtzman, J. A., et al., 1998, AJ, 115, 1946
- Kent, S. M., 1992, ApJ, 387, 181
- Mao, S., & Paczynski, B., 1991, ApJ, 374, L37
- Miller, G. E., & Scalo, J. M., 1979, ApJS, 41, 513
- Ortiz, R., & Lépine, J. R. D., 1993, A&A, 279, 90
- Paczynski, B., 1996, ARA&A, 34, 419
- Peale, S., 1997, Icarus 127, 269
- Reid, M., 1993, ARA&A, 31, 345
- Schneider, P., Ehlers, J., & Falco, E. E., 1992, Gravitational Lenses, (Springer: New York), p. 319
- Tiede, G. P., Frogel, J. A., & Terndrup, D. M., 1995, AJ, 110, 2788
- Wainscoat R. J., Cohen, M., Volk, K., Walker, H. J., Schwartz, D. E., 1992, ApJSS, 83, 111
- Wambsganss, J., 1997, MNRAS, 284, 172
- Wambsganss, J., & Kubas, D., 2000, in preparation
- Wardle, M. & Yusef-Zadeh, F., 1992, ApJ, 387, L65

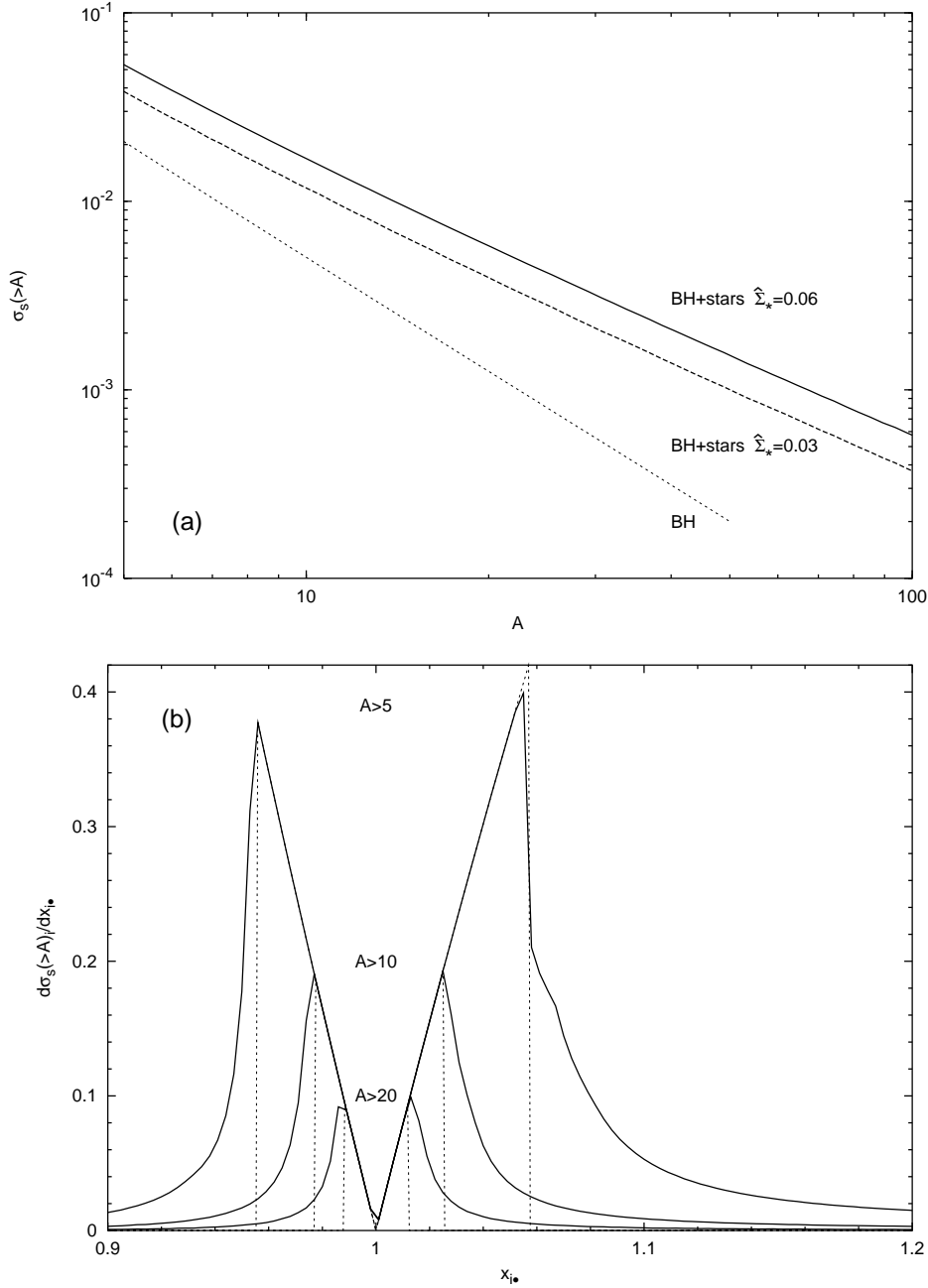


Fig. 1.— (a) The mean source area for amplification by more than  $A$  by the BH and stars of an image in the inner  $2\theta_E$ . The stellar lens surface density is assumed to be  $\Sigma_* = \hat{\Sigma}_* x^{-1/2}$  ( $\alpha = 3/2$ ). The magnification by the BH alone is compared with that for the BH and two different values of  $\hat{\Sigma}_*$ . (b) The differential source area per annulus in the lens plane that is magnified by more than  $A$  assuming  $\hat{\Sigma}_* = 0.03$ . The case of a BH and stars (full lines) is compared to the contribution from the BH alone (dashed lines) for three threshold values of  $A$ .

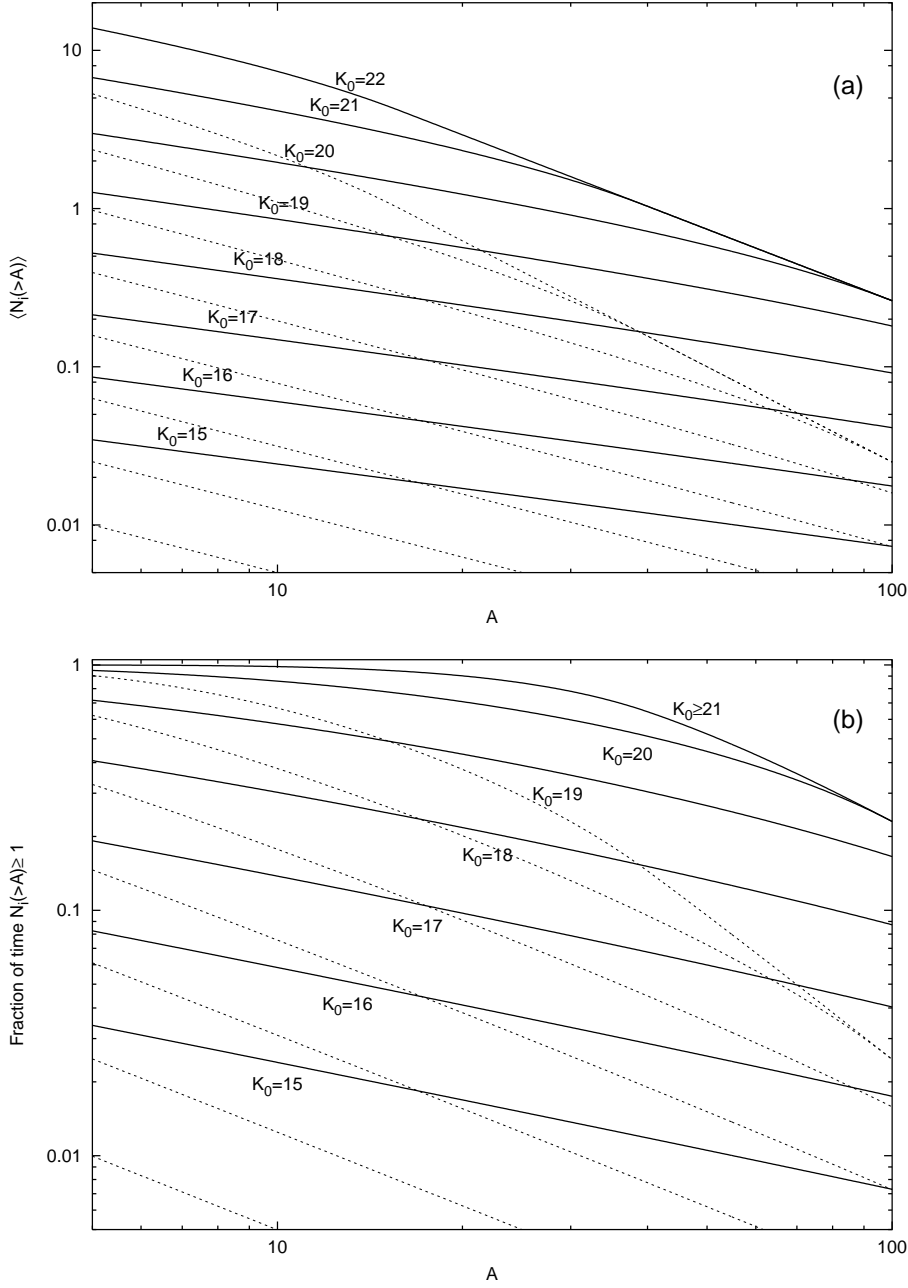


Fig. 2.— (a) The average number of lensed images magnified by more than  $A$  that will be observed in the inner  $2\theta_E$  with a limiting  $K$ -band magnitude  $K_0$ . (b) The fraction of time that at least one lensed image magnified by more than  $A$ , will be observed in the inner  $2\theta_E$  with a limiting  $K$ -band magnitude  $K_0$ . In both figures, the KLF of Eq. (11) is assumed. The labeled solid lines are for  $\widehat{\Sigma}_* = 0.06$  and the unlabeled dotted lines, which follow the same  $K_0$  order, are for the BH alone.

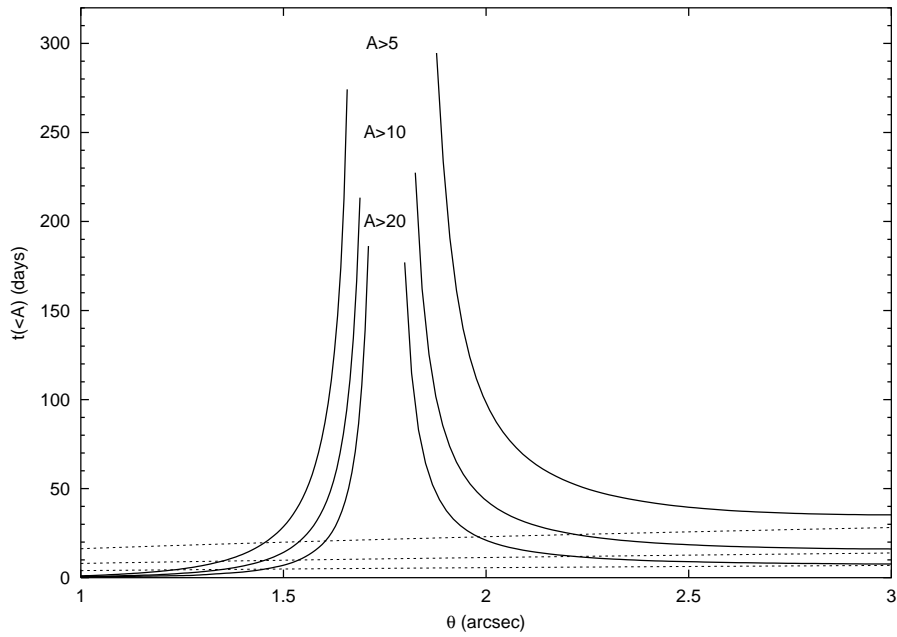


Fig. 3.— The typical duration of a microlensing event for a stationary source at infinity by a solar mass lens [assuming the mean rms velocity of Eq. (13)], as a function of angular separation  $\theta = x_i \bullet \theta_E$  from SgrA\* ( $\theta_E = 1.75''$ ). Curves are shown for different magnification values  $A$ , comparing stars in the shear field of the BH (full lines) with isolated stars moving at the same velocity (dashed lines).